EXPERIMENTAL AND NUMERICAL STUDY OF THIN WALL LIQUID FILM SPREADING ON A HEATING SURFACE.

S. Giroud-Garapon*, G. Heid*, G. Lavergne*, and O. Simonin**
Stephane.Giroud-Garapon@onecert.fr
***ONERA - Centre de Toulouse-DMAE,**
2 avenue E. BELIN, BP 4025
31055 Toulouse Cedex 4 – France.
(S. Giroud-Garapon, G. Heid, G. Lavergne.)
****Institut de Mécanique des Fluides de Toulouse,**
Allée du Professeur Camille Soula
31400 Toulouse – France.
(O. Simonin)

Abstract.

Wall spray interactions play an important role in the combustion efficiency prediction of turbojet or ramjet. They generate complex physical phenomena such as rebound onto wall or rebound onto wetted surface, splashing, deposition, film formation, film streaming and film atomization. ONERA/DMAE has been working on these subjects for few years, and some wall-drop interaction models have been developed and integrated into CFD-industrial-codes.

In order to improve this work, a basic experimental study has been performed to analyze wall liquid film inside a combustion chamber. In this way, an experiment was built in a rectangular experimental wind tunnel with transparent walls in order to visualize and to analyze, with non-intrusive techniques based on laser trace displacement, the liquid film flowing on a flame-holder (300-700K) put on the bottom wall of the tunnel. The liquid film is entrained by a co-flowing air stream. The air velocity is ranging from 30 to 100 m/s.

The aim of the present experiment is to create firstly an experimental data-base on wall liquid film behaviour in terms of thickness, velocity and surface instabilities evolution considering different aerodynamic and wall thermal regimes. Secondly, liquid film atomisation at the flame-holder trailing edge was analysed with a MALVERN system in order to establish an experimental model of liquid film disintegration. These two physical phenomena will be then integrated in CFD-codes.

A liquid film model is developed in parallel for integration in ONERA CFD-codes using an Euler-explicit scheme. This model is based on 2D Navier-Stokes incompressible equations. The formulation of the governing equations takes into account the different physical phenomena occurring all around the thin liquid film. These phenomena are wall film formation by an impinging spray, film transport governed by mass and momentum equations considering wall and air flow interaction in terms of heat transfer and shear stress, drop impact, and evaporation.

Introduction.

Combustion chamber development and their performance study are a field in which numerical simulations play an important role. The improvement of the predictions begins with the development of more and more sophisticated models, in order to take into account the maximum of physical phenomena. Nowadays, some of these phenomena associated with wall/spray interactions are always little or badly modeled and make that the drop size resulting from these impacts is not very well known. It is nevertheless this drop size which is important during the combustion chamber efficiency calculation.

Numerical simulation improvements require the development of sophistical models. Some of them are already used in ONERA CFD codes, such as dispersion, combustion, secondary break-up (*see* Fig. 1). The purpose of this study is to pursue this effort by focusing on the streaming and the pulverization of a liquid film (*see* Fig.2). In this way, a fine experimental study is organized. A film thickness measurement system was set up in order to establish an experimental data base for the validation of the numerical model developed in parallel.

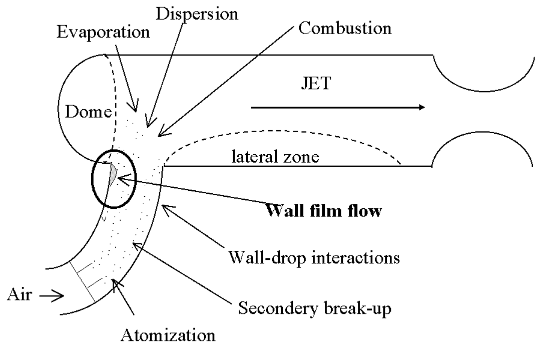

Figure 1. Physical phenomena in a combustion chamber.

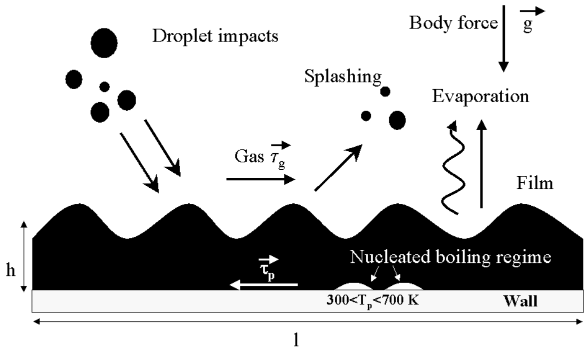

Figure 2. Film streaming.

Experimental set up.

A basic experimental study has been performed in order to analyze wall liquid film inside a combustion chamber (Giroud-Garapon *et al*. [1]). This is a cold flow experiment (*see* Fig. 3), where a liquid film is flowing on a flame holder put on the bottom wall of the tunnel. The experiment has a rectangular geometry with a cross section of 100*100 mm^2 with transparent walls. The air velocity is ranging from 30 to 100 m/s.

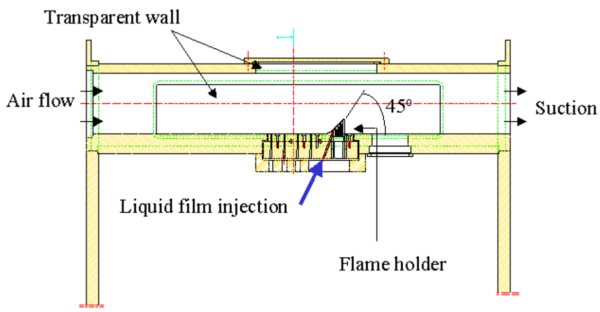

Figure 3. Wind tunnel.

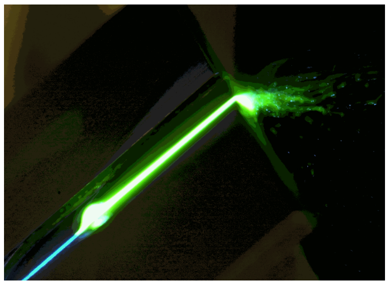

Figure 4. Film streaming.

Ethanol enriched with fluoresceine is used as fuel. The liquid injection is controlled by a flow metering unit. The liquid emerges from a pipe with a diameter of 1 mm (*see* Fig 4). Afterwards the film flow is canalized in a groove of 1mm depth and 10 mm width. It is streaming on the flame holder which temperature should be fixed from 300 K to 700 K by an element heating controlled electronically.

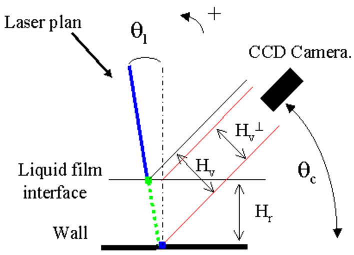

$$H_r = \frac{H_v}{Cos(\theta_c)}\left[\frac{1}{1+Tan(\theta_c)*Tan(\theta_L)}\right]$$

Figure 5. Measurement principle.

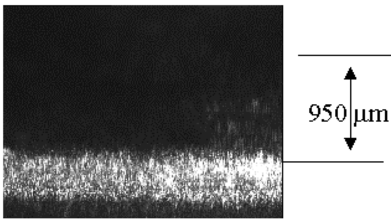

Figure 6. Image without film H_r=0.

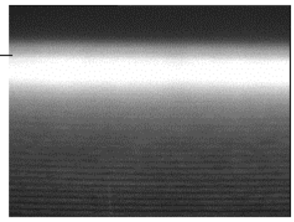

Figure 7. Image with liquid film H_r=950 µm.

The film thickness is measured with a non-intrusive technique based on the laser trace displacement at the liquid film interface (*see* Fig 5). Indeed, when the film thickness varies, the trace of the laser plan is moving. Thus, it is enough to know the optical magnification used to obtain the film thickness. For that purpose, laser trace positions obtained with and without liquid film are compared (*see* Figs 6 and 7). This technique gives only the thickness of the film, so its velocity has to be estimated using flow rate conservation.

The following figures present the first results obtained in cold condition (*see* Figs 8 and 9). We notice that the film thickness logically decreases from the upstream to the downstream. On the other hand, a more important flow logically leads to a thicker film.

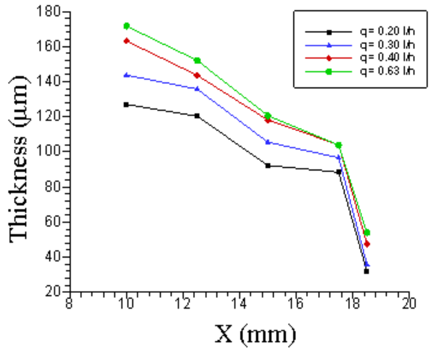

Figure 8. Axial film thickness measured for 30 m/s air flow rate.

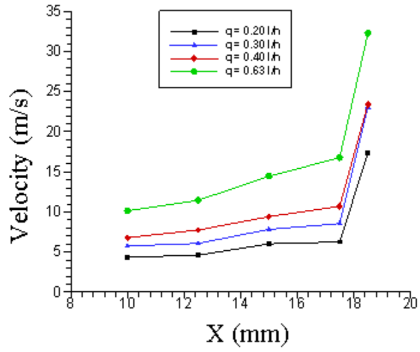

Figure 9. Film velocity calculated for 30 m/s air flow rate.

Numerical tools.

Numerical thin liquid film study and its integration in industrial CFD Codes are not easy. Indeed, the common mesh size generally used at the wall is about 1 mm. That's why this type of mesh is not sufficient to characterize finely thin liquid film.

Two different approaches can be used to simulate wall liquid film, the *eulerian* approach or the *lagrangian* approach. The *lagrangian* approach considers the film as a carrier phase of liquid particles. This method is used in ONERA CFD Codes but it does not seem to be adequated for the study of a continuous phase.

The *eulerian* approach considers the liquid phase as a continuous phase. Here an eulerian approach based on Foucart et al [2] [3] models is used. This is the indirect *eulerian* method where the film is likened to a surface entity. This model presents two advantages:

- The film is 2D. Indeed, the thickness of the film is virtual that is to say, calculated in the same way as other thermodynamic variables,
- The gas volume at the wall remains unchanged. Only conditions in aerodynamic limits are modified by the presence of the film.

Thus, Navier-stoke equations are reduced to the following integral two dimensional forms.

Continuity equation.

$$\underbrace{\frac{dV_D}{dt}}_{\{1\}} + \underbrace{\oint_{\partial A} h(\vec{u}.\vec{n})^* \, dl}_{\{2\}} = S_m \qquad (1)$$

In this equation, {1} is the time derivative of the liquid volume V_D. {2} is the convective volume term which expresses the flow rate across the boundary lines δD. The source term S_m represents the rate of fuel at the liquid-gas interface due to impinging droplets, splashing droplets, and film evaporation or condensation [2].

Momentum equation.

$$\underbrace{\frac{d\vec{u}_D V_D}{dt}}_{\{1\}} + \underbrace{\oint_{\partial A_p} h[\vec{u}_D.\vec{u}_D]\,.\vec{n}dl}_{\{2\}} = \underbrace{\frac{-1}{\rho_l}\oint_{\partial A_p} hp_D\vec{n}dl}_{\{3\}} + \underbrace{\vec{\tau}_g}_{\{4\}} - \underbrace{\vec{\tau}_w}_{\{5\}} + \underbrace{\vec{g}V_D}_{\{6\}} + \underbrace{\vec{S}_{Mvt}}_{\{7\}} \tag{2}$$

In the left hand side, {1} is the time derivative of the momentum and {2} is the convective momentum term. The first term in the right hand side {3} comes from pressure gradient which expression is given in [2]. The liquid-gas shear stress given by Foucart et al [2] [3] is modified in order to take into account the waviness of the film by introducing an equivalent sand grain roughness. Taking pattern from the work of Himmelsbach et al [4], this equivalent roughness is defined to:

$$K_s = 2.h\,.\psi \tag{3}$$

$$\psi = 0.735 + 0.009255\left[Pa^{-1}\right]\tau_s \tag{4}$$

Himmelsbach et al [4] found this correlation for ψ to give good results for the velocity profile of the gas phase in connection with a logarithmic law of the wall:

$$u^+ = \frac{1}{k'}\ln\left(y^+\right) + C(Re_{Ks}) \tag{5}$$

With:

$$Re_{Ks} = \frac{u_\tau .K_s}{\nu_w} \tag{6}$$

Three different regimes of film roughness may be identified leading to different values of $C(Re_{Ks})$

$$\begin{aligned}
C(Re_{Ks}) &= 5.15 && Re_{Ks} < 5.15\\
C(Re_{Ks}) &= 1.5497 + 19.1*\log(Re_{Ks}) && 5 \le Re_{Ks} \le 70\\
&\quad -14.4339*\left[\log(Re_{Ks})\right]^2 &&\\
&\quad +3.30869*\left[\log(Re_{Ks})\right]^3 &&\\
&\quad -\frac{1}{k'}\ln\left(Re_{Ks}\right) &&\\
C(Re_{Ks}) &= 8.5 - \frac{1}{k'}\ln\left(Re_{Ks}\right) && 70 < Re_{Ks}
\end{aligned} \tag{7}$$

These equations lead to a correction (τ_s’) of the wall shear stress given by the aerodynamics CFD code (τ_s).

$$\frac{1}{\sqrt{\tau_s'}} = \frac{1}{\sqrt{\tau_s}} + \frac{C(Re_{Ks}) - 5.15}{U_e\sqrt{\rho}} \tag{8}$$

Thus, the liquid-gas shear stress {4} is given by:

$$\vec{\tau}_g = \frac{A_w\vec{\tau}_s'}{\rho_l} \tag{9}$$

To compute the wall shear stress {5}, a laminar parabolic liquid velocity profile is assumed. Using a zero liquid velocity at the wall and the continuity of the velocity and shear at the interface give the following expression is obtain for the wall shear stress.

$$\vec{\tau}_w = 3\frac{\nu_l A_w \vec{U}_D}{h} - \frac{1}{2}\vec{\tau}_g \tag{10}$$

The two last terms are the body forces {6} and source force {7} which is given by [2].

Enthalpy equation.

$$\underbrace{\frac{d\rho_l c_p \vec{T}_D V_D}{dt}}_{\{1\}} + \underbrace{\oint_{\partial A_p} h\left[\rho_l c_p \vec{T}_D . \vec{u}\right]_h . \vec{n} dl}_{\{2\}} = \underbrace{\vec{J}_g}_{\{3\}} - \underbrace{\vec{J}_w}_{\{4\}} + \underbrace{\vec{S}_H}_{\{5\}} \tag{11}$$

Where {1} is the time derivative of the enthalpy, {2} is the convective enthalpy term, {3} is the gaz heat flux, {4} is the wall heat flux, and {5} is a source term due to the enthalpy supplied by impinging droplets. The gaz heat flux J_g is obtained using the interface condition:

$$\vec{J}_g = A_w j_g - S_v L \tag{12}$$

Where j_g is already given by the aerodynamic CFD code, S_v is a source term due to the film evaporation at the liquid gas interface. L is the liquid latent heat of vaporization. The wall heat flux J_p is calculated assuming a parabolic temperature profile. The following expression is then obtained:

$$J_p = 3 * \frac{k(T_D - T_w)}{\rho_l h} A_w - \frac{J_g}{2} \tag{13}$$

Experimental and numerical comparison.

In order to assess the accuracy of the film model, it is compared with Wittig [5] experiments (*see* Figs. 10 and 11). Comparisons presented (*see* Fig. 11) show a good agreement when the sand grain approach is used. Nevertheless other cases have to be tested in order to show the same level of agreement.

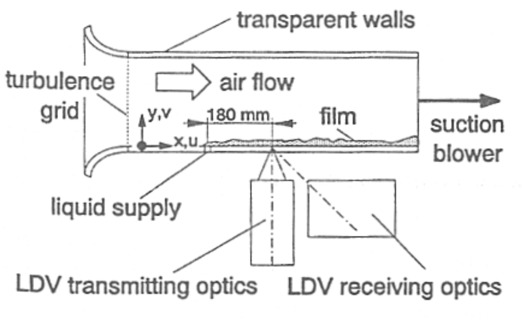

Figure 10. Wittig test section (U_g=30 m/s).

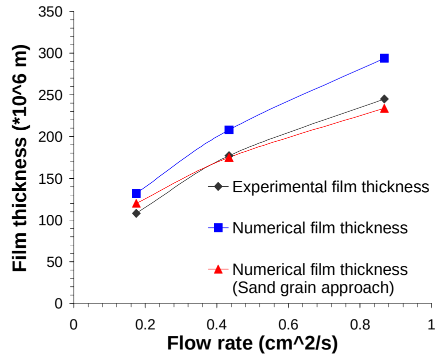

Figure 11. Comparisons between experimental results and numerical simulations.

Conclusion.

To avoid the cost and complexities of a full 3D computation, an integral film model is used. This model based on Foucart [2] work has been corrected in order to take into account the waviness of the film by introducing an equivalent sand grain roughness. This model is in course of validation with experimental results found in the literature as well as on those stemming from our experiment led in parallel. This experiment which is beginning, allowed us to validate an innovating film thickness measurement technique. Actually everything is in place to develop an experimental data base allowing the validation of this numerical code.

Nomenclature.

A	[m^2]	section
C	[var]	constant in logarithmic law
c_p	[$J.Kg^{-1}K^{-1}$]	specific heat
g	[$m.s^{-2}$]	body force
h	[m]	film thickness
Hv	[m]	film thickness saw by the CCD camera
$Hv^{\perp}$	[m]	film thickness saw by the CCD camera corrected
Hr	[m]	experimental film thickness
J	[$J.s^{-1}$]	heat flux
j	[$J.s^{-1}m^{-2}$]	heat flux give by CFD Code
K_s	[m]	equivalent Sand grain roughness
k	[$J.s^{-1}.m^{-1}.K^{-1}$]	thermal conductivity
k’	[var]	Von Karman constant
S_H	[$J.s^{-1}$]	enthalpy source term
S_m	[$m^3.s^{-1}$]	volume source term
S_{mvt}	[$m^4.s^{-2}$]	momentum source term
S_v	[$Kg.s^{-1}$]	evaporation source term
t	[s]	time
u	[$m.s^{-1}$]	velocity
u_τ	[$m.s^{-1}$]	shear stress velocity
u^+	[var]	non-dimensional film velocity
U_e	[$m.s^{-1}$]	gas velocity
V	[m^2]	volume
y^+	[var]	non-dimensional wall distance
μ	[$Kg.s^{-1}.m^{-1}$]	dynamic viscosity
ν	[$m^2.s^{-1}$]	cinematic viscosity
θ_c	[rad]	ccd camera angle
θ_l	[rad]	laser plane angle with the normal to the wall
ρ	[$Kg.m^{-3}$]	density
τ_s	[Pa]	shear stress given by CFD Code
τ_s’	[Pa]	shear stress given by CFD Code corrected
τ	[$m^4.s^{-2}$]	shear stress
ψ	[var]	efficiency factor of film roughness

Subscripts

D	control volume
g	gas
l	liquid film
w	wall

References.

[1] Giroud-Garapon, S., Heid, G., ”Modélisation de la combustion diphasique dans les statoréacteurs,” ONERA Laboratories Report No. 1/05604 DEFA/DMAE, 2002.

[2] Foucart, H., Habchi, C., Le Coz, J.F., and Baritaud, T., “Development of a three dimensional model of wall fuel liquid film for internal combustion engines”, *SAE 980133*, (1998).

[3] Foucart, H., Ph.D. Thesis, University of Rouen, France, 1998.

[4] Himmelsbach, J., Noll, B., and Wittig, S., “Experimental and numerical studies of evaporating wavy fuel films in turbulent air flow”, *Int. J. Heat Mass Transfer*, Vol. 37, No. 8, 1994, pp 1217-1226.

[5] Wittig, S., Elsaber, A., Samenfink, W., Ebner, J., Dullenkopf, K., “Velocity profiles in shear-driven liquid films: LDV- measurements”, LITS Universität Karlsruhe (TH), Germany, 1997